Power Electronic Systems
Laboratory

Proceedings of the 37th Annual Conference of the IEEE Industrial Electronics Society (IECON 2011), Melbourne, Australia, November 7-10, 2011.

High-Temperature (250 C / 500 F) 19'000 rpm BLDC Fan for Forced Air-Cooling of Advanced Automotive Power Electronics

B. Wrzecionko
A. Looser
J. W. Kolar
M. Casey

Eidgenössische Technische Hochschule Zürich
Swiss Federal Institute of Technology Zurich

High-Temperature (250 °C / 500 °F) 19'000 rpm BLDC Fan for Forced Air-Cooling of Advanced Automotive Power Electronics

Benjamin Wrzecionko, Andreas Looser and Johann W. Kolar
Power Electronic Systems Laboratory
ETH Zurich
Zurich, Switzerland
Email: wrzecionko@lem.ee.ethz.ch

Michael Casey
Institute of Thermal Turbomachinery
and Machinery Laboratory
University of Stuttgart
Stuttgart, Germany

***Abstract*—In an increasing number of application areas and industry sectors, such as the automotive, aerospace, military or oil and gas industry, a trend towards higher ambient temperature rating from 120 °C upward for electrical machines and power electronic converters can be observed. Forced air-cooling of power electronic converters offers reduced complexity of the cooling circuit compared to water-cooling. For high ambient temperature rated converters fans are required that withstand these temperatures and still feature performance comparable to standard conditions in order to still enable a high converter power density and efficiency. Commercially available fans for power electronics cooling are typically rated up to 75 °C, very rarely fans are specified up to 105 °C.**

In this paper, the electrical and mechanical design of a 40 mm × 40 mm × 28 mm fan is presented in detail that offers an operational temperature range up to 250 °C at the rated speed of 19'000 rpm and similar fluid dynamical performance in terms of static pressure and volume flow at 120 °C as commercial high performance fans at 20 °C. The 3-phase BLDC machine driving the fan is integrated into its hub and has got an input power of 15 W. The fan can be driven using a 3-phase inverter supplied from 12 V DC voltage with an inverter switching frequency of less than 1.3 kHz.

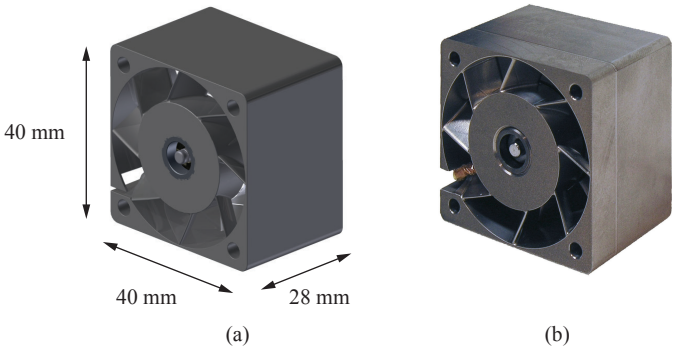

Fig. 1. CAD picture (a) and photograph (b) of high-temperature (250 °C / 500 °F) 19'000 rpm BLDC fan for forced air-cooling of advanced automotive power electronics.

I. Introduction

Automotive power electronic converters have substantially gained research and development interest triggered by the increasing market share of hybrid electric vehicles (HEVs). Compared to conventional drive concepts, where the vehicle is driven by an internal combustion engine (ICE) only and power electronic converters are solely found in auxiliary drives or power supplies, typically a series-connections of DC-DC and DC-AC converter(s) is used to drive the electrical machine(s) in the drive train of the HEV. Hence, the power level of automotive power electronic converters is currently increasing by orders of magnitude; the power level of a conventional alternator and its rectifier is below 5 kW for a passenger car [1], while the power level of the electrical machine can be as high as 160 kW as for the 2008 Lexus LS 600h [2].

The power electronic converters, especially the DC-AC drive inverters, are placed underneath the engine hood in the majority of today's HEVs, close to the electrical machine in order to transmit the high voltages of the inverter switched at high frequencies over short distances only. The electrical machine is positioned in close vicinity to the drive train components which it is mechanically coupled to such as the ICE and the gearbox. The ambient temperature in the engine compartment can reach 120 °C (and even higher values around 650 °C close to the exhaust system) [3], [4]. Today's automotive power electronic converters employ Silicon (Si) power semiconductors with an upper junction temperature limit between 150 °C and 175 °C. In order to establish a sufficiently large temperature difference between the Silicon (Si) power semiconductor junction and the ambient, the "ambient" temperature of the converter is artificially lowered by water-cooling using a water-glycol mixture with a maximum temperature around 50 °C to 70 °C, that is separated from the cooling circuit of the ICE [5], [6].

Using the wide band-gap power semiconductor Silicon Carbide (SiC) as well as novel joining and bonding technologies such as sintered silver die attachment and copper bonding, the junction temperature of the power semiconductors can be increased to values higher than 175 °C [7]. This allows to establish a sufficiently high temperature difference between the power semiconductor junction and the ambient temperature level, even if the ambient temperature of the converter is raised to 120 °C by using the water-glycol cooling

TABLE I
Overview over high temperature fan specifications.

Dimension	Value	Unit
Maximum Air Temperature	250	°C
Maximum Static Pressure	415	Pa
Maximum Volume Flow	0.88	m^3/min
Rotational Speed	19'000	min^{-1}
Electrical Input Power	15	W
Electrical Machine Type	3ph Brushless DC	
Nominal Input Terminal Voltage rms	7.7[1]	V
Nominal Input Phase Current rms	1.4	A
Nominal Electrical Input Frequency	1267	Hz
Mass	96	g

[1] Fan inverter DC input voltage of 12 V is sufficient to drive fan with rated speed at nominal operating point.

978-1-61284-972-0/11/$26.00 ©2011 IEEE

circuit of the ICE or by direct air-cooling using the ambient air underneath the engine hood [8]. With respect to cost and complexity of the cooling system, direct air-cooling appears as the superior solution as no pumps, water pipes and water-air heat exchangers are needed. A junction temperature around 250 °C for typical SiC power semiconductors at 120 °C ambient temperature has been calculated to be close to the optimum junction temperature with respect to chip utilization and power density for an 120 °C ambient-air-cooled DC-AC inverter [9].

With direct air-cooling of automotive power electronic converters at 120 °C ambient and 250 °C junction temperature, not only the power semiconductors and their packaging, but also the signal electronics, the passive components like DC-link capacitors as well as the components of the air-cooling system such as thermal interface materials, heat sinks and fans need to withstand these harsh temperature conditions. For the signal electronics and passives, a converter setup dealing with the challenges induced by 120 °C ambient and 250 °C junction temperature is shown in [8]. Thermally conductive interface materials are available up to 300 °C [10], heat sinks are typically made of aluminum or copper and thus withstand these temperatures as well.

With respect to the high temperature capability of available fans, the picture changes significantly: Most of the commercially available DC fans suitable for designing compact power electronic converters, i. e. those having a high pressurization and volume flow with respect to their volume, suffer from operating temperature limits below or equal 75 °C. The electrical and mechanical design of these fans might allow the manufacturer to test at and then specify for somewhat higher ambient temperatures with only slight component changes. Still, the lifetime of the ball bearings used in e. g. Sanyo Denki fans, some of which are very competitive in terms of high pressurization and volume flow with respect to their volume, is cut by half for each 15 °C ambient temperature rise and the maximum operating temperature is 105 °C [11].

Other fan manufacturers sell fans for electronic cooling with temperature ratings up to 90 °C but these fans suffer from larger size and poorer fluid dynamical performance compared to the Sanyo Denki models [12]. Other solutions available on the market are fans for ovens with recirculating air that do not have the electrical machine in the hub of the fan but have it placed externally to reduce the ambient temperature of the electrical machine. The fan is then driven by a belt or a shaft which results in a more bulky setup and available rotational speeds are typically lower.

High ambient temperature electrical machines needed for integration of the machine into the hub of the fan are also currently investigated in other application areas, especially in the aerospace and the offshore downhole industry. Research for expeditions to the Venus have yield switched reluctance machines for up to 540 °C, but they are designed for an operational lifetime of 50 days only [13]. Furthermore, deeper oil reservoirs are currently explored, where electrical submersible pumps are used to provide a continuous flow of oil up to the surface [14]. The electrical machines used in the pumps can withstand temperatures up to 218 °C [15].

In this paper, a high temperature brushless direct current (BLDC) machine fan withstanding an ambient temperature of 250 °C with a rotational speed of 19'000 rpm for forced air-cooling of advanced automotive power electronics is presented. The BLDC electrical machine driving the fan is integrated into the hub of the fan and thus can withstand 250 °C ambient temperatures as well. The power electronic inverter for the BLDC machine of the fan is realized on a separate PCB, that is part of the 120 °C ambient temperature rated DC-AC traction inverter [8].

The fluid dynamical performance of the fan in terms of static pressure and volume flow at the nominal ambient temperature of 120 °C for power electronic converters placed under the engine hood in HEVs is comparable to that of commercial high performance fans at their nominal ambient temperature of 20 °C. The 250 °C specification gives designers of high-junction-temperature SiC power electronic converters more freedom of arranging the converter components as the fans can also be placed on the air outlet side of the heat sink so that they draw the hot air out of the heat sink rather than blowing it into the heat sink. Then, a combination of both arrangements resulting in a setup consisting of one heat sink in the middle of two fans is of course also feasible.

It is shown in detail in the next section Section II, how the fan specifications such as the dimensions, fluid dynamical performance and machine characteristics are derived with respect to the needs induced by air-cooling of ultra compact automotive power electronic converters for high ambient temperatures. Subsequently, the design of the electrical machine and mechanical parts is carried out in Section III and Section IV, respectively.

II. Fan Specifications

A. Air-Cooling of Power Electronics

In general, the cooling system of a power electronic converter has to dissipate the power loss of lossy components within the converter via a thermally conductive path to the ambient with a thermal resistance R_{th} as low as possible. At the same time, the cooling system is required to have a volume V_{CS} as small as possible in order to facilitate a high power density of the converter, leading to the definition of the *cooling system performance index* (*CSPI*) which is the inverse of the product of R_{th} and V_{CS} [16].

Beside these crucial demands, standard requirements for technical systems apply also for power electronic cooling systems: low system complexity, manufacturing and maintenance cost, size, weight, power consumption, noise generation and performance invariance against deterioration or spread for standard factory models.

B. Air Flow Direction

The applicability of a certain fan for a forced air-cooling setup within a power electronic converter can be assessed based on the direction of the air flow it produces: Centrifugal or radial fans can hardly be integrated into a typical setup without modifications where lossy components, e. g. power semiconductors, are mounted on heat sinks with extruded fins. A modified centrifugal fan, that guides the radial air flow into a tangential direction, is called blower. These fans deliver high pressure and volume flow for a certain outlet cross-section of the fan compared to axial fans, but their overall volume is usually significantly larger.

The most common fans with the largest variety of models for power electronics cooling are diagonal and axial flow fans. The difference between both fans is that for diagonal fans the housing and sometimes also the blades are conical with a larger diameter at the fan outlet so that the air is guided not only in axial direction out of the fan but has also got a small radial velocity component. This allows the fan to produce higher pressure at a higher volume flow for the same size and power rating. It has to be mentioned though, that it is strongly dependent on the geometry of the heat sink attached to the fan outlet and the attachment itself (e. g. spacing between fan outlet and heat sink) whether the diagonal component of the air flow is utilized or whether the air is directed back into the axial direction by the heat sink. In fact, most fans that are referred to as "axial" are constructed

as slightly diagonal fans. Hence, in this paper the terminology will be the same as usual and these fans will be referred to as axial. Some of the axial fans have guide vanes at the outlet side of the housing to reduce the air spin produced by the rotating vanes.

Counter rotating axial fans are equipped with two rotors that rotate in opposite directions yielding a high pressurization. Optimizing the fin design of the heat sink for the use with such fans with respect to the thermal resistance of the heat sink leads to very thin fins with very small spacing in between them which makes the manufacturing process very expensive and is only available for small aspect ratios of fin height to fin thickness [16]. Therefore, the additional pressure does usually not pay off in terms of power density.

Hence, the high temperature fan in this paper is designed as a single stage axial flow fan with guide vanes.

C. Physical Dimensions

The length of the outlet cross-section edges of the high temperature fan is chosen with regard to ubiquitous applicability to 40 mm × 40 mm (*cf.* Fig. 1). This corresponds to the largest fans that are commercially available while still being below the size of one rack unit, which is $1\mathrm{U} = 1.75\,\mathrm{in} = 44.45\,\mathrm{mm}$. For reference purposes and the sake of compatibility, the axial length of the high temperature fan is chosen to 28 mm which equals the length of the in terms of static pressure over volume flow very competitive Sanyo Denki San Ace 40 GV [17].

D. Static Pressure vs. Volume Flow at Increased Ambient Temperatures

The fluid dynamic characteristic of a fan determines together with the heat sink fin and baseplate design the resulting thermal resistance $R_{\mathrm{th,HA}}$ from the heat sink surface with the lossy component mounted on to the ambient. It is usually given as a static difference in pressure Δp between the outlet and inlet side of the fan vs. its volume flow $\dot{V}$ for a certain rotational speed n of the fan rotor. This characteristic curve depends largely on the measurement conditions especially with respect to the air density, which is mainly given by air temperature and absolute air pressure. Fan manufacturers often measure the curve according to the standard AMCA 210-85, set by the Air Movement and Control Association (AMCA) International [18], [19]. The reference air temperature is set to $T_0 = 20\,^{\circ}\mathrm{C}$ and the absolute pressure to $1.013 \cdot 10^5\,\mathrm{Pa}$ [18]. In Fig. 2, the curve of the commercial high performance Sanyo Denki San Ace 40 GV is given as an example. As mentioned in Section I, the design target for the fluid dynamic performance of the high temperature fan at $T_1 = 120\,^{\circ}\mathrm{C}$ is to be equal or better than that of the San Ace 40 GV reference fan at T_0.

With increasing ambient temperature T, the air density ρ decreases according to the ideal gas law with absolute pressure p and the gas constant $R = 287.06\,\frac{\mathrm{J}}{\mathrm{kg \cdot K}}$ for dry air:

$$\rho = \frac{p}{R \cdot T} = \begin{cases} 1.20 \\ 0.90 \\ 0.67 \end{cases} \begin{matrix} \\ {}^{\mathrm{kg}}/_{\mathrm{m}^3} \\ \\ \end{matrix} \quad \text{for} \quad \begin{matrix} T = \ 20\,^{\circ}\mathrm{C} \\ T = 120\,^{\circ}\mathrm{C} \\ T = 250\,^{\circ}\mathrm{C} \end{matrix} \tag{1}$$

Within the operating temperature range of the fan, its speed control keeps the rotor speed constant. Even with varying air density, this leads to a constant volume flow $\dot{V}$ of the fan [20]

$$\dot{V} = \mathrm{const} \qquad \text{for} \qquad n = \mathrm{const}. \tag{2}$$

However, Δp as well as the shaft power P of the fan scale proportionally with ρ leading to an inversely proportional correlation with T for $n = \mathrm{const}$ [20]:

$$\frac{\Delta p}{\Delta p(T_0)} = \frac{P}{P(T_0)} = \frac{T_0}{T} = \begin{cases} 1 \\ 0.75 \\ 0.56 \end{cases} \quad \text{for} \quad \begin{matrix} T = \ 20\,^{\circ}\mathrm{C} \\ T = 120\,^{\circ}\mathrm{C} \\ T = 250\,^{\circ}\mathrm{C} \end{matrix} \tag{3}$$

The resulting curve $\Delta p(\dot{V})$ at $T_1 = 120\,^{\circ}\mathrm{C}$ for the example San Ace 40 GV fan is depicted in Fig. 2. Notice, that this is only a theoretical curve as this commercial fan cannot be operated at this elevated temperature (*cf.* Section I). With respect to the change in power, it has to be noted, that the input power of the fan may not decrease by the same amount as the shaft power does due to decreasing fan motor and inverter efficiency at higher temperatures.

The reduction in Δp caused by an increased temperature T_1 can be compensated by increasing the rotor speed of the fan from the speed $n_{\mathrm{RF}} = 16'500\,\mathrm{rpm}$ [17] of the San Ace 40 GV reference fan to n_{HTF} for the high temperature fan. To derive the exact correlation between n_{RF} and n_{HTF}, the following fan laws stating the relations for $T = \mathrm{const}$ can be used [21]:

$$\dot{V}_{\max} = k_1 \cdot n \cdot d^3 \tag{4}$$

$$\Delta p_{\max} = k_2 \cdot n^2 \cdot d^2 \tag{5}$$

$$P_{\mathrm{in}} = k_3 \cdot n^3 \cdot d^5 \tag{6}$$

The fan diameter is denoted by d, the input power by P_{in} and $k_i, i = 1..3$, represent factors of proportionality depending on the design of a specific fan. k_1 and k_2 vary only by a factor of two from one fan to another for most commercial fans [21]. Assuming a similar fluid dynamic design of the reference and the high temperature fan in terms of the fan dimensions as well as the rotor and stator guide vanes, k_1 and k_2, respectively, will be very similar for the two fans. In order to meet the fluid dynamic design target of the high temperature fan, the following constraint has to be fulfilled:

$$\Delta p_{\mathrm{HTF}}(T = T_1 = 120\,^{\circ}\mathrm{C}) \overset{!}{\geq} \Delta p_{\mathrm{RF}}(T = T_0 = 20\,^{\circ}\mathrm{C}) \tag{7}$$

It can be seen from (3) that $\Delta p_{\mathrm{HTF}}(T = T_0)$ of the new high temperature fan has to be ${}^{T_1}/_{T_0}$ times higher than $\Delta p_{\mathrm{RF}}(T = T_0)$ in order to meet (7). With (5), n_{HTF} can be calculated to

$$\begin{aligned} n_{\mathrm{HTF}} &= n_{\mathrm{RF}} \sqrt{\frac{\Delta p_{\max,\mathrm{HTF}}(T_0)}{\Delta p_{\max,\mathrm{RF}}(T_0)}} = n_{\mathrm{RF}} \sqrt{\frac{T_1}{T_0}} \\ &= 16'500\,\mathrm{rpm} \cdot \sqrt{\frac{393.15\,\mathrm{K}}{293.15\,\mathrm{K}}} \approx 19'000\,\mathrm{rpm}. \end{aligned} \tag{8}$$

According to (4), the increased speed n_{HTF} also influences the volume flow of the fan which increases linearly with increasing speed. The resulting curve $\Delta p(\dot{V})$ of the high temperature fan is shown in Fig. 2.

Furthermore, shaft power P is also increased for the high temperature fan as it scales with n^3 [20]. The rise in shaft power for the nominal operating point T_1 of the high temperature fan compared to the nominal operating point T_0 of the reference fan is not as high as expected from the cubic correlation as the temperature rise from T_0 to T_1 reduces the required shaft power according to (3). The exact increase in shaft power P_{HTF} for the high temperature fan can be

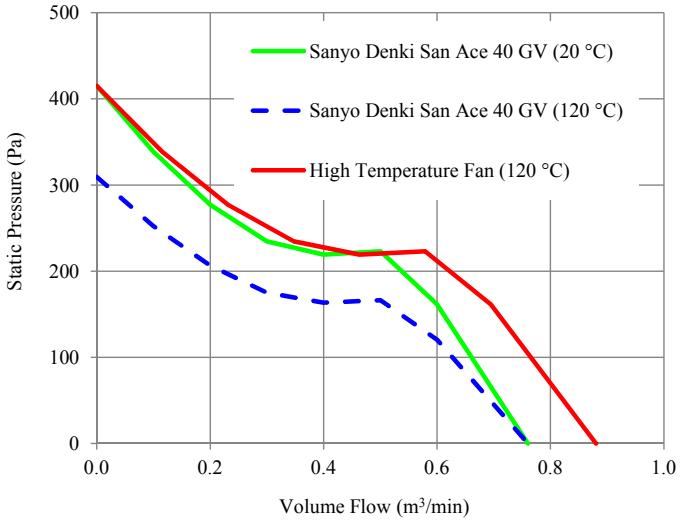

Fig. 2. Static pressure over volume flow curve for the Sanyo Denki San Ace 40 GV with 16'500 rpm fan as a competitive commercial reference at 20 °C (green line), its theoretical characteristic at 120 °C (dashed blue line) and the characteristic of the high temperature fan presented in this paper with 19'000 rpm at 120 °C (red line).

derived:

$$
\begin{aligned}
P_{\mathrm{HTF}}(T) &= P_{\mathrm{RF}}(T)\left(\frac{n_{\mathrm{HTF}}}{n_{\mathrm{RF}}}\right)^3 \qquad (9)\\
&= P_{\mathrm{RF}}(T_0)\left(\frac{n_{\mathrm{HTF}}}{n_{\mathrm{RF}}}\right)^3 \begin{cases} 1 & \text{for } T = 20\,^\circ\mathrm{C} \\ \frac{T_0}{T_1} & \text{for } T = 120\,^\circ\mathrm{C} \end{cases}\\
&= P_{\mathrm{RF}}(T_0) \begin{cases} \left(T_1/T_0\right)^{3/2} & \text{for } T = 20\,^\circ\mathrm{C} \\ \sqrt{T_1/T_0} & \text{for } T = 120\,^\circ\mathrm{C} \end{cases}\\
&= P_{\mathrm{RF}}(T_0) \begin{cases} 1.55 & \text{for } T = 20\,^\circ\mathrm{C} \\ 1.16 & \text{for } T = 120\,^\circ\mathrm{C} \end{cases}
\end{aligned}
$$

The shaft power $P_{\mathrm{RF}}(T_0)$ of the reference fan and thus the output power of its electrical machine is unknown, the input power $P_{\mathrm{in,RF}}$ is 10.1 W [17]. If a similar efficiency of the electrical machine for both fans is assumed, the required input power $P_{\mathrm{in,HTF}}$ of the high temperature fan can be specified to 15 W. This makes the operation of the high temperature fan at rated speed n_{HTF} even 100 °C below its nominal operating point, i. e. at standard conditions, possible.

E. Electrical Machine

1) General: In order to achieve a compact fan design (*cf.* Section II-A), the electrical machine has to be integrated into the hub of the high temperature fan. Hence, the machine must be able to withstand an ambient temperature of 250 °C plus the self-heating due to its losses. Typically, an internal fan motor is designed as a machine with an external rotor as this simplifies the mechanical construction and the usual drawbacks of external rotor machines such as higher rotational mass with a larger distance to the axis of rotation, both of which lead to a higher moment of inertia than for an internal rotor machine, are of less importance for fan operation where the moment of inertia smoothes a potential cogging torque and the speed control is not required to be highly dynamic.

The input power of the machine is determined in Section II-D to 15 W at its nominal operating point with a rated speed of 19'000 rpm. As this fan is designed for cooling of automotive power electronics, the machine should be able to be driven by an inverter supplied from a 12 V DC bus.

2) Machine Type: Possible types of electrical machines can be based on either electric or magnetic fields. With respect to the machine dimensions with an outer diameter of 23 mm and an axial length of 10 mm (restricted by the mechanical design, *cf.* Section IV), those using magnetic fields for the electromechanical energy conversion are preferable due to a higher energy and force density [22]. They include induction, permanent magnet, switched reluctance or conventional DC machines with brushes or brushless DC machines. At first sight, induction and switched reluctance machines appear as favorable choices for harsh environment conditions as they are regarded as very robust machines without need for expensive and temperature dependent permanent magnets.

Still, it has to be considered, that the motor torque is generated by the stator and rotor flux components which can be both electromagnetically excited or electromagnetically and permanent magnetically excited. The flux density caused by a permanent magnet is constant for varying machine dimensions while the rated current of an electrical machine decreases proportionally to decreasing machine dimensions. Hence, for small drives with diameters of less than 100 mm like in this case, machines with permanent magnet, i. e. DC or synchronous machines, are the favorable choice if a high power density is needed [23].

Conventional DC machines with brushes can be driven from a constant DC voltage source in their nominal operating point so that no additional inverter is necessary which is advantageous especially at such harsh environment conditions. Still, the brushes suffer from significant wear and affect the reliability. If the fan is required to be speed controlled in order to make sure that the fluid dynamic performance varies only little over the complete temperature range of approx. 300 K, additional controls are needed. Furthermore, a DC machine with brushes designed as with an external rotor requires additional mechanical effort.

Hence, the integrated machine of the high temperature fan will be designed as a BLDC machine which is constructed as permanent magnet synchronous machines (the magnetic design can be slightly different to make the rotor produce a rectangular rather than a sinusoidal back EMF) but is driven with (in case of a 3-phase machine) 120 ° phase-shifted rectangular voltages instead of pulse-width modulated voltages forming a sinusoidal current waveform. This gives a slightly higher torque and allows to reduce the switching frequency of the inverter and thus its losses which is in a 120 °C ambient temperature environment with only 55 °C margin to the upper junction temperature limit of Si power semiconductors a significant advantage.

3) Number of Phases: 1-phase BLDC machines need less complex inverters than machines with a higher phase count. Either an H-bridge inverter with two high-side switches and four switches in total supplying a single winding or two low-side switches supplying two separate windings connected in anti-series can be employed. This half-wave configuration needs only two switches, but the copper utilization is lower than for the H-bridge as each winding conducts only one half-wave. A significant drawback of 1-phase machines is the asymmetry of the magnetic design needed to make sure that the machine can be put into rotation from any rotor position.

2-phase BLDC machines having symmetric windings can be started from any rotor angle, but the drive inverter complexity is basically multiplied by two for the H-bridge or half-wave solution. It is also possible to use a single half-bridge for two windings if the midpoint of the series-connected windings is connected to the midpoint of supply. This solution though requires a supply voltage balancing and cuts the voltage that can be applied to the windings in half.

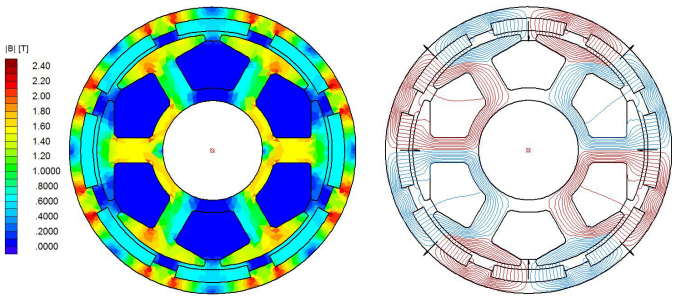

(a) (b)

Fig. 3. Flux density distribution of the BLDC machine under full load condition (a) and magnetic field lines under no load condition (b).

A 3-phase BLDC machine appears as a reasonable compromise between the request for a symmetric machine design on the one hand and low drive effort on the other hand as the H-bridge of the 1-phase machine needs to be extended by only one more bridge leg. Furthermore, a large variety of gate drivers for 3-phase inverters and control ICs for 3-phase BLDC is available as 3-phase BLDC machines are widely used in industry. Hence, the BLDC machine for the high temperature fan will be designed as a 3-phase machine.

III. Electrical Machine Design

A. Windings

The isolation of the windings has to withstand the sum of the maximum operating temperature and the temperature rise due to ohmic losses in the windings. High temperature versions of conventional enameled copper wire can continuously withstand temperatures up to only 245 °C [24], [25]. A solution is copper wire, that is clad by nickel for increased oxidation resistance and coated by ceramic for electrical insulation. It can withstand temperatures up to 700 °C for more than 1'000 h and 425 °C for more than 5'000 h [26].

The resulting specific electrical resistance ρ_{CuNi} of the nickel clad copper wire can be calculated, if the fractions of nickel and copper are given. The Kulgrid 28 wire used for this setup consists of $y_{\mathrm{Ni}} = 27\%$ nickel and $y_{\mathrm{Cu}} = 1 - y_{\mathrm{Ni}} = 73\%$ [27]. As the density of nickel is with $8.880\,{}^{\mathrm{g}}/_{\mathrm{cm}^3}$ less than 1% smaller than that of copper with $8.960\,{}^{\mathrm{g}}/_{\mathrm{cm}^3}$ at 20 °C [28], it is of negligible interest for the calculation of ρ_{CuNi} whether the volume or mass fractions are given. At higher temperatures, the densities match even better as copper expands with $16.4 \cdot 10^{-6}\,{}^{1}/_{\mathrm{K}}$ and nickel with $13.1 \cdot 10^{-6}\,{}^{1}/_{\mathrm{K}}$ only.

If the wire cross-section is ideal such that a round copper conductor is encapsulated with a nickel clad of constant thickness, the following formula and results can be calculated from Ohm's law of parallel conductors using the specific electrical resistances $\rho_{\mathrm{Cu}} = 16.9\,\mathrm{n\Omega \cdot m}$ and $\rho_{\mathrm{Ni}} = 71.9\,\mathrm{n\Omega \cdot m}$ of copper and nickel, respectively, as well as their coefficients of the linear increase in resistivity with temperature, $\alpha_{\mathrm{Cu}} = 0.0039\,{}^{1}/_{\mathrm{K}}$ and $\alpha_{\mathrm{Ni}} = 0.0066\,{}^{1}/_{\mathrm{K}}$ [28]:

$$\begin{aligned}\rho_{\mathrm{CuNi}} &= \frac{\rho_{\mathrm{Cu}} \cdot \rho_{\mathrm{Ni}}}{y_{\mathrm{Ni}} \cdot \rho_{\mathrm{Cu}} + y_{\mathrm{Cu}} \cdot \rho_{\mathrm{Ni}}} \\ &= \begin{cases} 21.3\,\mathrm{n\Omega \cdot m} \\ 41.3\,\mathrm{n\Omega \cdot m} \end{cases} \text{for} \begin{array}{l} T = 20\,^{\circ}\mathrm{C} \\ T = 250\,^{\circ}\mathrm{C} \end{array} \\ &= \begin{cases} 1.26 \cdot \rho_{\mathrm{Cu}}(20\,^{\circ}\mathrm{C}) \\ 2.44 \cdot \rho_{\mathrm{Cu}}(20\,^{\circ}\mathrm{C}) \\ 1.29 \cdot \rho_{\mathrm{Cu}}(250\,^{\circ}\mathrm{C}) \end{cases} \text{for} \begin{array}{l} T = 20\,^{\circ}\mathrm{C} \\ T = 250\,^{\circ}\mathrm{C} \\ T = 250\,^{\circ}\mathrm{C} \end{array} \end{aligned} \tag{10}$$

(The conductivity of the wire is further affected by diffusion of nickel into the copper core. After 500 h operation at 600 °C, the resistivity increase by another 25% for a wire with a fraction of 27% nickel [29].)

To avoid cracks of the ceramic insulation, the minimum bending radius of the ceramic coated nickel clad copper wire has to be at minimum 10-times larger than the outer diameter of the wire, which influences the design of the stator iron sheet package significantly (*cf.* Section III-B). For this setup, a wire with an external diameter of 0.1 mm is used.

B. Stator Iron Sheet Package

The minimum bending radius of the ceramic coated wire (*cf.* Section III-A) means for the stator iron sheet package, that the tooth width has to be equal or larger than 2 mm. As higher numbers of teeth with a width of 2 mm would drastically reduce the winding area, the package is designed with 6 teeth. The number of poles is chosen to 8, as with a lower number, the yoke would increase in radial thickness and the winding factor of 0.87 for this combination is better or equally good than for 10 or more poles.

Eligible materials include Silicon-Iron, Nickel-Iron or Cobalt-Iron. Silicon-Iron is the cheapest material but has a lower saturation flux density and higher losses. Lowest losses and highest permeabilities offer Nickel-Iron alloys. Highest flux density and thus highest torque and power density are possible with Cobalt-Iron which makes it the favorable material for the high temperature fan.

Vacoflux 48 by Vacuumschmelze has got a very narrow hysteresis loop ($H_{\mathrm{C}} < 40\,{}^{\mathrm{A}}/_{\mathrm{m}}$) and a high saturation flux density of $B_{\mathrm{S}} = 2.35\,\mathrm{T}$. The Curie temperature is $T_{\mathrm{C}} = 950\,^{\circ}\mathrm{C}$ and the coefficient of thermal expansion is $\alpha_{\mathrm{CTE}} = 9.5 \cdot {}^{10^{-6}}/_{\mathrm{K}}$. For this setup, 100 individual 0.1 mm thick sheets are chosen leading to an axial length of the machine of 10 mm. The sheets are laminated together for easier manufacturing. The adhesive used by Vacuumschmelze is only specified up to 190 °C, at higher temperatures it looses its adhesive effect and transforms into carbon which influences the behavior of the package: The temperature of the material causes the hysteresis loop to shear so that the magnetic permeability decreases and the coercitivity slightly increases. This leads to slightly higher losses in the range of +5% for a temperature of 300 °C.

C. Permanent Magnets

The permanent magnets used in the high temperature fan need to have a sufficiently high remanence induction B_{r} and coercive force H_{C} at 250 °C. Hard magnetic materials with a high energetic product include Neodymium-Iron-Boron (NdFeB) and Samarium-Cobalt ($SmCo_5$ and Sm_2Co_{17}). For high temperature applications, the only possible material is SmCo. (Aluminium-Nickel-Cobalt, AlNiCo, is also possible, but has got a much lower energy product than SmCo.) Arnold Magnetics offers Recoma main grades an Recoma HT Magnets, the latter for operating temperatures up to 520 °C. For the high temperature fan, Recoma HT 420 magnets with a remanence of 0.9 T and an intrinsic coercive force of $1100\,{}^{\mathrm{kA}}/_{\mathrm{m}}$ at 250 °C are deployed. The maximum demagnetization force applied to the magnets is $290\,{}^{\mathrm{kA}}/_{\mathrm{m}}$.

The magnets do not need to be protected against corrosion at 300 °C. At temperatures higher than 400 °C they can be either packaged in a steel housing, which increases the length of the air gap of the machine, or coated with Aluminium (up to 500 °C) or with Nickel (up to 550 °C).

The magnet segments can be fit into the yoke and are kept only by their magnetic force. Alternatively, they can be laminated into the yoke with adhesive based on Silicon or Ceramics. These adhesives though cannot absorb high thermo-mechanical stresses. The thickness of the magnets should not be thinner than the actual 1 mm in order to make sure they do not break during manufacturing. If smaller

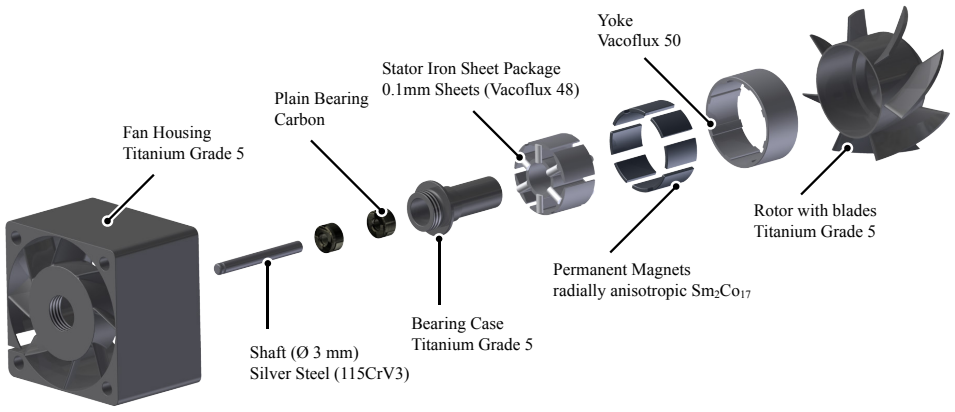

Fig. 4. Exploded view drawing of high-temperature (250 °C / 500 °F) 19'000 rpm BLDC fan for forced air-cooling of advanced automotive power electronics.

thicknesses need to be realized though, the magnets can be mounted into the yoke and then ground to the desired thickness.

D. Yoke

The geometry of the yoke is chosen such that the flux density has a maximum value of 2 T. The air-gap is 0.3 mm. The material should have a relative permeability of 500 at this point for minimizing the resistance of the magnetic path. Furthermore, the CTE should be close to that of the rotor as the yoke is directly fit into the rotor. The afore mentioned Cobalt-Iron alloy Vacoflux 50 by Vacuumschmelze fulfills these criteria.

IV. Mechanics Design

In this section, the mechanical design of the high temperature fan, especially the choice of different technologies such as the bearing technology and the selection of the design concept as well as the materials are described, each with respect to the high temperature rating, the resulting thermal expansion and reduced strength of the materials and other constraints such as magnetic fields of the machine potentially causing eddy current losses.

The exploded view drawing in Fig. 4 shows the assembly of the individual fan components. The fan housing is the structural part of the fan. On the outlet side, there is a center borehole with inside thread. The bearing case is screwed into that hole. The plain bearings are shrunk into the bearing case and carry the shaft. The stator iron sheet package is shrunk onto the bearing case and ceramic coated copper windings are wound onto the stator. The permanent magnets of the electrical machine are mounted in the steel yoke which is then shrunk into the rotor. The rotor itself is shrunk onto the shaft at the fan inlet. The axial position of the rotor is determined by the magnetic force of the permanent magnets. Additionally, it can be fixed with respect to the plain bearing on the fan outlet using a small spring and a snap ring.

A. Shaft

The shaft is carried by plain bearings and hence, it is very important that the thermal expansion of the shaft is close to that of the plain bearings, which is mainly determined by the bearing case (*cf.* Section IV-B). Otherwise for certain temperatures within the operating temperature range, either the bearing clearance has to be chosen very high resulting in high vibrations or the shaft gets stuck in the bearing.

In order to achieve a low coefficient of friction between the shaft and the bearing, the material is required to be harder than 40 HRC. Well suited material is steel (apart from Chromium-Nickel- and austenitic steel), e. g. Chromium, nitrified or hard-chromium plated steel, or hard metal. Not suited is Aluminium and its alloys or non-ferrous metal. The roughness of the material should lower than $1\,\mu\mathrm{m}$ for low friction [30]. Reduction of the surface roughness can be achieved by surface finishing and polishing. The diameter of the shaft is determined by the mechanical load due to unbalance of the rotor, desired vibration reduction and resonance of the rotating shaft.

The shaft for this high temperature fan is made of a cylindrical pin, the material of this pin is steel 115CrV3 (also called steel 1.2210). It is hardened to $60 \pm 2\,\mathrm{HRC}$ and its roughness class is N6, corresponding to a roughness depth of $R_\mathrm{a} < 0.8\,\mu\mathrm{m}$. The CTE of the material is $13.7 \cdot 10^{-6}\,{}^1\!/_\mathrm{K}$ for a temperature rise from 20 °C to 300 °C. The diameter of the pin is 3m6 and it will be cut to a length 27.5 mm, i. e. the length of the shaft is reduced by 0.5 mm compared to the overall length of the fan in order to make sure that no rotating part overlaps the housing.

B. Bearing

Generally, the bearings can be realized as:

- Roller bearing
- Static or dynamic air bearing
- Magnetically levitated bearing
- Plain bearing

Magnetically levitated and air bearings are very complex, costly and not as compact as plain or roller bearings. Roller bearings need lubrication, and this is usually only used for temperatures below 200 °C. Some special greases are available up to 260 °C and very rarely greases for higher temperatures are applicable.

The more cost effective and easier solution for the high temperature bearing is the plain bearing. Different materials are available for standard conditions, e. g. metal or solid polymer, mono-, bimetallic or sintered bearings, fibre-reinforced plastic composite, bronze or (artificial) carbon. Most materials are eliminated due to the high temperature the bearings are exposed to (the bearing losses make the bearing heat up to even higher temperatures), only bronze and carbon are suitable.

The carbon bearing is the only suited plain bearing for this purpose, if the high rim speed of the shaft is taken into account, which can be calculated to

$$v = \omega r = 2\pi \cdot 19'000\,\mathrm{rpm} \cdot 1.5\,\mathrm{mm} = 3.0\,{}^\mathrm{m}\!/_\mathrm{s}. \qquad (11)$$

The dimensions of the bearing are determined by the requirements of the technology, i. e. the difference between the inner and outer

radius is usually not less than 3 mm. For applications that have to be highly compact, the difference can be reduced to 2 mm because of the very small shaft diameter of 3 mm. This leads to an outer diameter of 7 mm and the axial length of the bearing is chosen to 4 mm.

The inner diameter of the bearing is given by the outer diameter of the shaft (3m6, i. e. $3\,\mathrm{mm}\ \binom{+0.008}{+0.002}$, which will be reduced by approx. $6\,\mu\mathrm{m}$ by polishing the shaft). The inner diameter is furthermore influenced by the bearing clearance, that is given for dry operation from 0.3% to 0.5% of the shaft diameter [30]. Lower clearances cause higher friction and thus higher losses, higher clearance values cause higher vibrations. Also, the thermal expansion of shaft (*cf.* Section IV-A) and bearing has to be taken account when determining the inner diameter of the bearing. The bearing has a CTE of $5 \cdot 10^{-6}\,{}^{1}/_{\mathrm{K}}$ which is comparably low, but is shrunk into the bearing case at a temperature that is 150 °C higher than the maximum operating temperature and therefore its thermal expansion is given by the bearing case (*cf.* Section IV-C).

C. Bearing Case

The material for the bearing case is required to have a CTE similar to the shaft, because the the bearing expands just as its case does and similar to the CTE of the stator iron sheet package that is shrunk onto the casing in order to avoid high thermal stresses.

Furthermore, the material has to be non-magnetic (i. e. a relative permeability of $\mu_r \leq 1.0$, that is also maintained after cold working) in order to make sure that the time varying magnetic flux density in the stator is solely conducted by the stator iron sheet package and hence no eddy current losses in the bearing case occur.

The yield strength up to the maximum operating temperature should be as high as possible because the carbon plain bearings are shrunk into the case. A high Young's Modulus makes sure, that the case even with a wall thickness of 0.5 mm at the inlet bearing is not widened excessively after shrinking in of the bearings. This is important because the stator iron sheet package has to be shrunk onto the bearing case after mounting the bearings as the sheet package is not recommended to be exposed to higher temperatures than 400 °C which are necessary to shrink the bearing in.

Titanium is available in many different alloys. The American organization ASTM International classifies 35 grades of different alloys. The most common grade is Titanium Grade 5 (also named by the material number 3.7164) which fulfills these requirements. Its CTE is $9.6 \cdot 10^{-6}\,{}^{1}/_{\mathrm{K}}$.

The shape of the casing is defined by its function: It is screwed into the fan housing and thus needs a stopper to control the length of the screwing. The step on the outer diameter is needed to have a stopper for the stator iron sheet package when shrunk onto the case. The outer diameter is with 8 mm as small as possible — the difference between inner radius at the bearing collet and the outer radius of the case is only 0.5 mm. The length of the case is 24 mm, mainly given by the 28 mm overall length of the fan, again 0.5 mm clearance and 3.5 mm shrink fit of rotor and shaft.

D. Rotor

The hub (24 mm outside) and blade (37 mm) diameter of the rotor as well as the blade shape are given by the fluid dynamical requirements (*cf.* Section II-D). The clearance between the rotor blades and fan housing is chosen to 0.5 mm due to manufacturing tolerances.

The material for the rotor must have high yield strength at high operating temperatures and a high resistance against fatigue cracks because of the high dynamic load caused by the rotations. The rotor

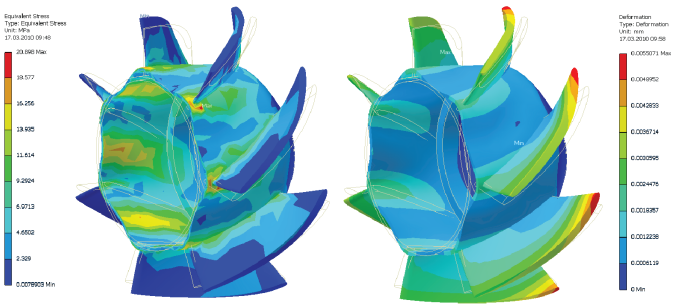

(a) (b)

Fig. 5. FEM simulation of rotor maximum stress (a) and deformation (b) at 300 °C. A safety margin of more than 20 for the maximum stress is included for the Titanium Grade 5 rotor.

is manufactured of Titanium Grade 5, just as the bearing case. The wall thickness is chosen to 0.5 mm as a trade-off between electrical machine diameter that has to be maximized and mechanical strength at high temperatures. It can be seen from the FEM simulation in Fig. 5 that the areas of highest load are at the transitions between the inner cylinder and the blades. The maximum stress of 20 MPa is more than a factor of 20 below the yield strength of Titanium Grade 5 at 300 °C. The maximum deformation is less than $6\,\mu\mathrm{m}$.

E. Fan Housing

The stator guide vanes direct the air flow in a more axial direction to increase the efficiency of the heat sink. The material for the stator should have a CTE close to the CTE of the bearing case in order to have a similar thermal expansion when the bearing case is screwed into the housing and hence, the bearing case is also made of Titanium Grade 5. For easier manufacturing of the housing, it is produced in two parts: The first part containing the guide vanes has got an axial length of 7 mm, the second part contains the boring for the rotor. These two parts are laser beam welded, as can be seen in Fig. 1(b).

V. Conclusion

In this paper, first the upcoming quest for 120 °C rated forced air-cooled power electronic converters in HEVs is motivated by showing the advantages of placing the converters as a part of the vehicles drive train underneath the engine hood. This creates the need for fans having a competitive fluid dynamic performance which are currently not commercially available at this temperature level. For certain cooling system setups in power electronic converters employing novel SiC semiconductors with elevated junction temperatures, these fans are required to operate up to 250 °C.

First, it is shown how the pressurization of the fan decreases at elevated temperatures and how the rotational speed can be increased to 19'000 rpm to compensate this decline. Then, special focus is put on the design of the integrated BLDC machine for an ambient temperature of 250 °C, including magnetic material selection (Sm_2Co_{17} permanent magnets for the rotor and Co-Fe sheets for the stator package) and choice of ceramic coated Ni-Cu windings introducing further constraints due to their minimum bending radius. The mechanical design of the fan for 250 °C operation and rim speeds up to $180\,{}^{\mathrm{m}}/_{\mathrm{min}}$ with plain bearings is conducted. The selection of the materials for the different fan components has been done based on the evaluation of the material stresses, the material strength at 250 °C and the thermal expansion at an operating temperature range of 300 K.

REFERENCES

[1] R. Schöttle and G. Threin, "Electrical power supply systems: present and future," *VDI Berichte*, vol. 1547, pp. 449–475, 2000.

[2] FreedomCAR and Vehicle Technologies Program, "Plug-in hybrid electric vehicle R&D plan," U. S. Department of Energy, Working Draft, Jun. 2007. [Online]. Available: http://www1.eere.energy.gov/vehiclesandfuels/pdfs/program/phev_rd_plan_june_2007.pdf

[3] F. Renken and R. Knorr, "High temperature electronic for future hybrid powertrain application," in *Proc. European Conference on Power Electronics and Applications (EPE 2005)*, Dresden, Germany, Sep. 11–14, 2005. [Online]. Available: http://ieeexplore.ieee.org/stamp/stamp.jsp?tp=&arnumber=1665959

[4] S. Pischinger, M. Pischinger, H. Kemper, and S. Christiaens, "The challenges of system integration of the hybrid electric powertrain," in *Fachtagungsberichte VDE Kongress*, Aachen, Germany, Oct. 23–25, 2006.

[5] V. Pickert, H. Cheng, L. Pritchard, and D. J. Atkinson, "An experimental and computational study of water cooled heatsinks for HEV's," in *5th IET International Conference on Power Electronics, Machines and Drives (PEMD 2010)*, Brighton, UK, Apr. 19–21, 2010. [Online]. Available: http://ieeexplore.ieee.org/stamp/stamp.jsp?tp=&arnumber=5522477

[6] C. W. Ayers, J. C. Conklin, J. S. Hsu, and K. T. Lowe, "A unique approach to power electronics and motor cooling in a hybrid electric vehicle environment," in *IEEE Vehicle Power and Propulsion Conference (VPPC 2007)*, Arlington, TX, USA, Sep. 9–12, 2007, pp. 102–106. [Online]. Available: http://ieeexplore.ieee.org/stamp/stamp.jsp?tp=&arnumber=4544107

[7] J. M. Hornberger, E. Cilio, B. McPherson, R. M. Schupbach, and M. A. H. Lostetter, A. B., "A fully integrated 300 °C, 4 kw, 3-phase, SiC motor drive module," in *Proc. IEEE Power Electronics Specialists Conference (PESC 2007)*, Orlando, FL, USA, Jun. 17–21, 2007, pp. 1048–1053. [Online]. Available: http://ieeexplore.ieee.org/stamp/stamp.jsp?tp=&arnumber=4342136

[8] D. Bortis, B. Wrzecionko, and J. W. Kolar, "A 120 °C ambient temperature forced air-cooled normally-off SiC JFET automotive inverter system," in *Twenty-Sixth Annual IEEE Applied Power Electronics Conference and Exposition (APEC 2011)*, Ft. Worth, TX, USA, Mar. 6–10, 2011, pp. 1282–1289. [Online]. Available: http://ieeexplore.ieee.org/stamp/stamp.jsp?tp=&arnumber=5744758

[9] B. Wrzecionko, J. Biela, and J. W. Kolar, "SiC power semiconductors in HEVs: Influence of junction temperature on power density, chip utilization and efficiency," in *35th Annual Conference of the IEEE Industrial Electronics Society (IECON 2009)*, Porto, Portugal, 3–5, 2009, pp. 3834–3841. [Online]. Available: http://ieeexplore.ieee.org/stamp/stamp.jsp?tp=&arnumber=5415122

[10] *Thermal Navigator*, HALA Contec GmbH & Co. KG, Alte Landstraße 23, 85521 Ottobrunn, Germany, Oct. 2010. [Online]. Available: http://www.hala-tec.com/mod_use/dokumente/Thermal-Navigator_en.pdf

[11] *Cooling Systems - Technical Material*, Sanyo Denki Co., Ltd., 1-15-1, Kita-otsuka, Toshima-ku, Tokyo 170-8451, Japan. [Online]. Available: http://db.sanyodenki.co.jp/product_db_e/coolingfan/pdf/e_spec.pdf

[12] *High Temperature Fans*, EVG Elektro-Vertriebs-Gesellschaft Martens GmbH & Co. KG, Trompeterallee 244-246, 41189 Mönchengladbach, Germany. [Online]. Available: http://www.evg.de/kataloge/En/EVG_1E10-english-022.pdf

[13] G. A. Landis, "Robotic exploration of the surface and atmosphere of Venus," *Acta Astronautica*, vol. 59, no. 7, pp. 570–579, 2006. [Online]. Available: http://www.sciencedirect.com/science/article/B6V1N-4K7NHFP-2/2/c996e7c5f080cad50baf43360c0289e9

[14] A. König, "High temperature DC-to-DC converters for downhole applications," Ph.D. dissertation, RWTH Aachen University, Aachen, Germany, Jun. 2009.

[15] Schlumberger, "REDA hotline high temperature ESP systems," 2007. [Online]. Available: http://www.slb.com/~/media/Files/artificial_lift/brochures/hotline_br.ashx

[16] U. Drofenik, G. Laimer, and J. W. Kolar, "Theoretical converter power density limits for forced convection cooling," in *Proceedings of the International PCIM Europe 2005 Conference*, Nuremberg, Germany, Jun. 2005, pp. 608–619. [Online]. Available: www.pes.ee.ethz.ch/uploads/tx_ethpublications/drofenik_PCIM05.pdf

[17] *San Ace 40 GV*, Sanyo Denki Co., Ltd., 1-15-1, Kita-otsuka, Toshima-ku, Tokyo 170-8451, Japan. [Online]. Available: http://db.sanyodenki.co.jp/product_db/cooling/dcfan/group_pdf/1247013350.pdf

[18] G. Tan, "Fundamentals of brushless DC axial cooling fans," Sanyo Denki Co., Ltd., 468 Amapola Avenue, Torrance, California, 90501, USA, Tech. Rep., Mar. 2008. [Online]. Available: http://www.newark.com/pdfs/techarticles/sanyo/fundamentals_brushlessDCcoolingFans.pdf

[19] ebm Industries, Inc., "Motor design, quality and performance are critical to reliable operation of fans & blowers," ebm Industries, Inc., Tech. Rep., 1999. [Online]. Available: http://www.ebmpapst.us/pdfs/motor.pdf

[20] W. Wagner, *Lufttechnische Anlagen: Ventilatoren und Ventilatoranlagen*, 2nd ed. Würzburg, Germany: Vogel Buchverlag, 1997.

[21] U. Drofenik and J. W. Kolar, "Thermal power density barriers of converter systems," in *Proc. of the 5th International Conference on Integrated Power Systems (CIPS 2008)*, Nuremberg, Germany, Mar. 11–13, 2008. [Online]. Available: http://ieeexplore.ieee.org/stamp/stamp.jsp?tp=&arnumber=5755678

[22] P. L. Chapman and P. T. Krein, "Micromotor technology: electric drive designer's perspective," in *Conference Record of the Thirty-Sixth IEEE Industry Applications Conference (IAS 2001)*, vol. 3, Chicago, IL, USA, Sep. 30 – Oct. 4, 2001, pp. 1978–1983. [Online]. Available: http://ieeexplore.ieee.org/stamp/stamp.jsp?tp=&arnumber=955899

[23] U. Kafader and J. Schulze, "Similarity relations in electromagnetic motors - limitations and consequences for the design of small DC motors," in *9th International Conference on New Actuators (ACTUATOR 2004)*, Bremen, Germany, Jun. 14–16, 2004, pp. 309–312.

[24] Elektrisola. (2011, Sep.) Enamelled copper wire acc to IEC - Europe. Online. [Online]. Available: http://www.elektrisola.com/enamelled-wire/enamelled-wire-types/iec/europe.html

[25] Pack Feindrähte. (2011, Sep.) Technical data table for fine wires. Online. [Online]. Available: http://www.pack-feindraehte.de/en/technical_data/fine_enamelled_copper_wires/magnet_wires.html

[26] Karl Schupp AG, *Winding wires with ceramic insulation*, V 2.2 ed., Wilhofstrasse 3, 8125 Zollikerberg, Switzerland. [Online]. Available: http://schupp.ch/gb/LTKR_ceramic_wires.htm

[27] *Ceramawire High Temperature Magnet Wire Technical Specifications*, Ceramawire, 786 Pitts Chapel Rd. , Elizabeth City, NC 27909, USA. [Online]. Available: http://www.ceramawire.com/ceramaTechspec.pdf

[28] R. B. Ross, *Metallic materials specification handbook*, 4th ed. Chapman & Hall, 2-6 Boundary Row, London SE1 8HN, UK, 1992.

[29] J. R. Howell, "Composite wires for operation as electrical conductors at elevated temperatures," in *Seventh Annual Wire and Cable Symposium*, Ashbury Park, NJ, USA, Dec. 2–4, 1958. [Online]. Available: http://handle.dtic.mil/100.2/AD656291

[30] GGT Gleittechnik AG, *Gleitlager aus Kohlenstoff*, 12g/10 ed., Postfach 164, Meierskappelstrasse 3, 6043 Küssnacht am Rigi, Switzerland, Dec. 2010. [Online]. Available: www.gleitlager.ch/upload/GGT_Gleitlager%20aus%20Kohlenstoff_V2.pdf